The Impact of Halftone Screen on Color Graininess

Chunghui Kuo and Yee Ng; Eastman Kodak; Rochester, NY, USA

Abstract

Color graininess is one of the most important artifacts affecting image quality. Previous studies have indicated that it is necessary to remove the screen signal on the scanned amplitude-modulated, AM, screen before adopting any granularity metric to achieve satisfactory correlation between the objective measurement and subjective evaluation, indicating the AM halftone screen has no effect on the perceived graininess. Nonetheless, the inherent characteristics of FM halftone screens with pseudorandom dot placement transforms the frequency content of the screen signal from spikes to a distribution across the spatial frequency domain. The objective of this experiment is to conduct a visual experiment comparing the perceived graininess on patches with various color generated by various types of AM and FM screens. Correlated with an unified objective granularity metric, we can evaluate the impact of various halftone screens on color graininess, and verify the assertion that the periodic screen signal is independent from the perceived graininess.

Introduction

Color graininess is one of the most important artifacts affecting image quality. However, the current international standard, ISO13660, only addresses the graininess of binary monochromatic patches in the perceptually nonuniform reflective density space without considering the impact of halftone screen. Previous studies have indicated that it is necessary to remove the screen signal on the scanned amplitude-modulated, **AM**, halftone screen before adopting any granularity metric to achieve satisfactory correlation between the objective measurement and subjective evaluation. This means that the **AM** halftone screen has no effect on the perceived graininess. We have extended the graininess metric on the color patches generated by the **AM** halftone screen to the **CIELAB** color space using the flatbed scanner as an efficient measurement device. Recently the frequency modulated, **FM**, halftone screen has become more popular with the perception that it is less affected by image Morié, and more capable to render detail information. Nonetheless, the inherent characteristics of pseudorandom dot placement have transformed the frequency content of the screen signal from spikes to a distribution across the spatial frequency domain. As a result, the granularity and **FM** halftone screen signals becomes indistinguishable in the spatial frequency domain as well as in the human perception. The objective of this experiment is to conduct a visual experiment comparing the perceived graininess on color patches generated by various types of **AM** and **FM** halftone screens, and correlate with an unified objective granularity metric quantifying the perceived color graininess without the influence of various types of halftone screens.

The challenge we face in this study is two fold. First is to devise a robust screen removal algorithm which can automatically adapt to the input scanned image and removes only the periodic, **AM**, halftone screen signals. The other task is to design an objective color granularity metric which can appropriately incorporate the **FM** halftone screen signals into the perceived graininess. Because the flatbed scanner is used in this study for its efficiency and the capability of capturing large print sample areas with fine detail, calibrating the flatbed scanner for every different set of colorants adopted in each printed sample is essential to ensure the accuracy of the color transformation from scanner device values to **CIELAB** color space [1, 2]. We adopt the space variant color screen removing algorithm based on *Short Time Fourier Transform* to remove periodic color **AM** halftone signals [3]. Assume the distribution of the logarithmic magnitude of the color granularity signal in the spatial frequency domain can be approximated as two separable signals: a slow-varying two dimensional signal and a white gaussian noise with zero mean, and a hard thresholding technique can adaptively identify and remove all periodic **AM** halftone signal without affecting other signal components [4]. Because there is no intention to redefine the spatial frequency range governing the granularity, the sampling algorithm of our proposed objective color granularity metric follows the original *ISO13660* method; however, we should note that the original method only operates in the binary monochrome reflection density space without considering the impact of various types color halftone signal [5]. Assuming the viewing distance being 0.3 meter and the lower limit in spatial frequency domain being 0.4 cycle/mm, the average color contrast sensitivity function indicates that the perceived color graininess is dominated by the noise in luminance perception [1]. This hypothesis will further be verified by our visual experiment.

In the visual experiment, we select 6 color patches from each halftone combination including cluster dot **AM**, hybrid **AM/FM**, coarse **FM**, and fine **FM** halftone screens from inkjet, electrophtography and offset printing processes. Each descreened color patch is first transformed to the **CIELAB** color space according to the corresponding scanner calibration function before estimating the associated color granularity.

Proposed Algorithm

Periodic Color Halftone Removal

Let the scanned image $I(x,y|r,g,b)$ be decomposed into three components: the actual image, $I_o(x,y|r,g,b)$, the halftone screen image, $I_s(x,y|r,g,b)$, and the imaging noise, $I_g(x,y|r,g,b)$, where $I_s(x,y|r,g,b)$ can be resulted from **AM**, **FM** or hybrid **AM/FM** halftone screens. $I_g(x,y|r,g,b)$ contains color granularity, mottle and other artifacts, which could come from the original imaging process as well as the printing process. The objective of the periodic color halftone removing algorithm is to only remove $I_s^{AM}(x,y|r,g,b)$; thus, we can formulate this problem as a binary hypotheses decision problem. Let H_0 and H_1 be two hypotheses:

$$H_0 \quad = \quad I_o + I_g + \zeta \times I_s^{FM}$$

$$H_1 = I_o + I_g + \zeta \times I_s^{FM} + I_s^{AM}$$

, where $\zeta = 0$ when no **FM** halftone signal exists, and $\zeta = 1$ when the **FM** halftone screen signal is present. The *Short Time Fourier Transform*, *STFT*, approach is adopted where the scanned image is decomposed into overlapping blocks. I_o can be further approximated as a low-pass filtered version of $I(x,y|r,g,b)$, I_o^i, within each block with cutoff frequency being 50dpi [3]. We denote $I_h(x,y|r,g,b) = I - I_o^i$. Therefore, we can rewrite H_0 and H_1 as follows by subtracting I_o^i from both scenarios:

$$H_0' = I_g + \zeta \times I_s^{FM}$$
$$H_1' = I_g + \zeta \times I_s^{FM} + I_s^{AM}.$$

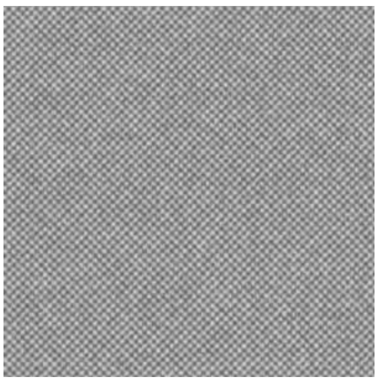

Figure 1. AM Halftone Scanned Image

The spectrum of the **FM** halftone screen signal spreads across the entire spatial frequency domain to avoid creating image Morié; thus, it is not separable from I_g in the spatial frequency domain. Consequently, by transforming to the spatial frequency domain, we can combine $\bar{I}_g(w_x,w_y|r,g,b) + \zeta \times \bar{I}_s^{FM}(w_x,w_y|r,g,b)$ as $\bar{I}_g^{FM}(w_x,w_y|r,g,b)$, and revise two hypotheses in the following:

$$\bar{H}_0 = \bar{I}_g^{FM}(w_x,w_y|r,g,b)$$
$$\bar{H}_1 = \bar{I}_g^{FM}(w_x,w_y|r,g,b) + \bar{I}_s^{AM}(w_x,w_y|r,g,b).$$

Let's assume that the logarithm of the magnitude of $\bar{I}_g^{FM}(w_x,w_y|r,g,b)$ in the null hypothesis $\bar{H}_0$ is composed of two separable signals: a slow-varying two dimensional signal, S_g, and a white Gaussian noise signal, $N(0,\sigma)$, with zero mean and σ standard deviation. Note that there exist constraints when a real signal is transformed to the spatial frequency domain, such as *Conjugate Symmetry*:

$$\bar{I}(w_x,w_y) = (\bar{I}(-w_x,-w_y))^*. \quad (1)$$

We have shown that a two dimensional spline functional satisfying constraint (1) can effective approximate S_g [3]. As a result, the binary hypotheses problem can be finalized as follows:

$$\bar{H}_0' = N(0,\sigma)$$
$$\bar{H}_1' = N(0,\sigma) + \bar{I}_s^{AM}(w_x,w_y|r,g,b).$$

Let

$$\|\bar{I}_r(w_x,w_y|r,g,b)\| = \log\|\bar{I}_h(w_x,w_y|r,g,b)\| - S_g, \quad (2)$$

and $\bar{I}_s^{AM}(w_x,w_y|r,g,b)$ can be estimated by the following hard-thresholding algorithm:

$$\bar{I}_s^{AM}(w_x,w_y) = 0, \; if \; \|\bar{I}_r(w_x,w_y)\| < \delta \quad (3)$$
$$\bar{I}_s^{AM}(w_x,w_y) = \bar{I}_r(w_x,w_y), \; if \; \|\bar{I}_r(w_x,w_y)\| \geq \delta, \quad (4)$$

where δ can be determined from $\|\bar{I}_r(w_x,w_y)\|$. Denote $\hat{\sigma}_r$ as the estimated standard deviation of $\|\bar{I}_r(w_x,w_y)\|$, and our current choice of $\delta = 3\hat{\sigma}_r$. The image with the **AM** color halftone screens removed can be easily obtained as follows:

$$I_d(x,y,r,g,b) = I(x,y|r,g,b) - I_r^{AM}(x,y|r,g,b). \quad (5)$$

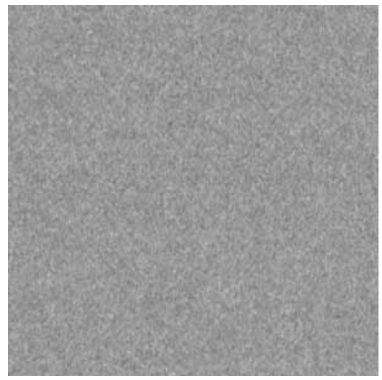

Figure 2. AM Halftone Processed Image

Objective Color Granularity Metric

In this study, we follow the definition of granularity in the frequency domain provided by *ISO13660* to be higher than 0.4 cycle/mm [5]. Thus, we adopt the same granularity sampling method: the image is divided as nonoverlapping blocks with size 1.27×1.27 mm, and total sampling area is at least 12.7×12.7 mm, i.e., there exists at least 10×10 sampling blocks. Assuming the viewing distance is 0.3 meter, and this results in an approximately 2 cycle/degree lower bound in the valid spatial frequency domain relating to the perceived graininess. The spatial contrast sensitivity functions of human beings for luminance and chromatic contrast indicate that chromatic contrast sensitivities are much lower than the luminance contrast sensitivity [6]. As a result, we can assume that the perceived color graininess is dominated by the perceived high frequency noise in luminance. Different from the granularity metric suggested by *ISO13660* which operates in the reflection density space, we propose to first transform the obtained $I_d(x,y|r,g,b)$ to the **CIELAB** color space respectively via the appropriate scanner calibration function. Different from the reflection density space suggested by *ISO13660*, the objective color granularity metric operates in the luminance space. Let τ be the standard deviation in each block, and the color granularity, G_c^L, can be computed as

$$G_c^L = \sqrt{\mathbf{E}\{\tau_i^2\}} \quad (6)$$

Visual Experiment and Data Analysis

Figure 1, 4, and 6 illustrate the **AM**, coarse **FM** and fine **FM** color halftone scanned images respectively. The one dimensional spatial frequency components of the coarse and fine **FM** halftone signals is shown in Figure 3 where the dominant frequency component of the fine **FM** signal is approximately 50% higher than that of coarse **FM** signal. The images processed by the proposed **AM** color halftone removing algorithm are shown in Figure 2, 5, and 7. All images were scanned with 800dpi resolution. It can be readily seen that the **AM** halftone signal is clearly removed while all other signals, including the coarse and fine **FM** halftone screen, are well preserved. The scanned and processed fine **FM** as shown in Figure 6 and 7 halftone images appear almost identical. Nonetheless, under close inspection, the security yellow dot pattern occurred in the original scanned fine **FM** halftone image in Figure 6 becomes blurred after processed by the algorithm, although it is very difficult to perceive. We believe that it is caused by the long tail in the frequency domain of a *rect* function representing a single dot in one dimension, where the *rect* function is defined as follows:

$$\begin{aligned} rect(x) &= 1 \quad if \ |x| < 1/2 \\ rect(x) &= 0 \quad otherwise. \end{aligned}$$

However, this deficiency of the **AM** halftone removing algorithm have only minimal impact, and won't affect the following color granularity computation.

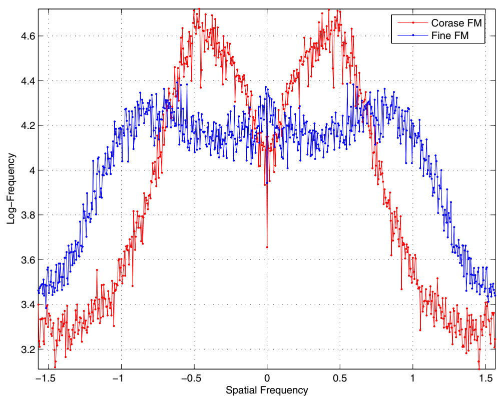

Figure 3. *One-Dimensional spatial frequency responses of coarse and fine FM halftone screens*

Figure 4. *Coarse FM Halftone Scanned Image*

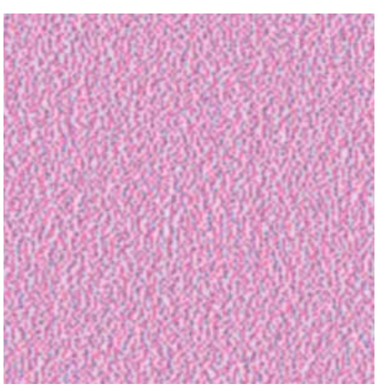

Figure 5. *Coarse FM Halftone Processed Image*

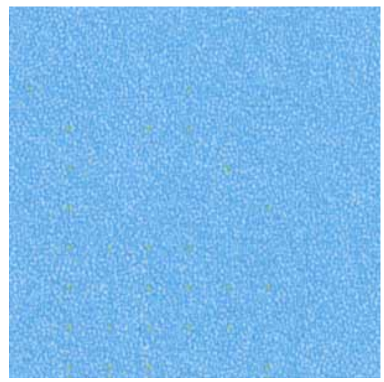

Figure 6. *Fine FM Halftone Scanned Image*

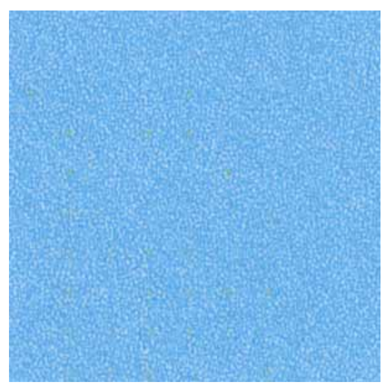

Figure 7. *Fine FM Halftone Processed Image*

Seven halftone/printing process combinations are included in this experiment, and there exists 6 color patches for each case. Fifteen observers participated in this experiment, and the standard graphic art viewing condition with D50 illumination is adopted. Two anchor prints are selected based on our previous study [1]. This experiment includes color patches with **AM**, hybrid **AM/FM**, coarse **FM** and fine **FM** halftone screens, and the adopted printing processes include inkjet, electrophotography, and offset press. Observers rank one patch at a time under the graphic art standard illumination **D50** with a number based on the comparison of two predetermined anchor patches, which are defined to have visual graininess as 20 and 80 respectively. Observers are allowed to penalize a target without an upper limit in the perceived graininess as suggested by the magnitude estimation visual evaluation method. The objective is to minimize the compressive nature of the visual response when an upper limit is imposed during a psychophysical experiment.

Figure 8 shows the computed objective granularity and the averaged visual responses. The highest and lowest graininess score for each color patch are excluded from the average operation. The relationship between the objective granularity metric, G, and the perceived color graininess, VG, can be described as follows:

$$VG = 9.08 + 48.94 \log(G). \quad (7)$$

The resulted R^2 value is 0.91. The derived logarithmic function indicates that the *Fechner's law* is capable of explaining the nonlinear physical metric and the subjective perception relationship, where the perceptual sensitivity in color graininess decreases with increasing granularity (*Weber's law*) [6].

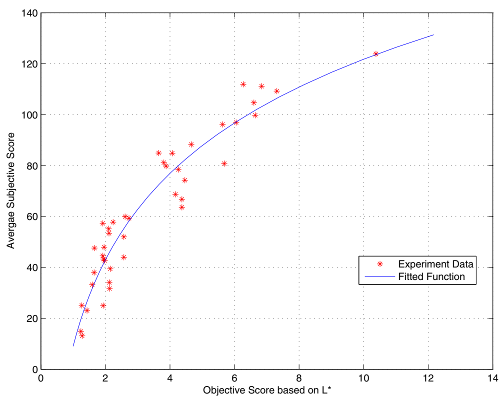

Figure 8. *Visual experiment data and the fitted curve*

Compare with the linear model we derived previously [1], and we can see that the dynamic range of the measured color granularity in this experiment is three times larger. As a result, the compressive nature of *Weber's law* becomes apparent in this study. Since the midpoint of the computed color granularity was approximately 2 in the previous study, we can easily derive the gradient of VG to be 24.47 from Equation 7. This is very close to the slope of the previous linear model as shown below:

$$VG = 23.16 \times G - 3.6. \quad (8)$$

Because the basic *Fechner's law* governing human perception response can sufficiently explain the relation between the proposed objective color granularity metric and the average visual score, we can reach the same conclusion as previous study on monochromatic halftone prints that the periodic **AM** halftone signal does not contribute to the perceived color graininess [7]. However, all other types of halftone signals, **FM** or hybrid **AM/FM**, will contribute to the perceived graininess. This explains why the images rendered with **FM** halftone screens is usually perceived as being noisier than otherwise rendered with **AM** halftone screens.

Conclusion

We extend the study on color graininess to include various types of halftone screens including **AM** and **FM** halftone screens. The visual experiment contains 42 color patches generated via Inkjet, Electrophotography and Offset press, and the magnitude estimation with two anchor print samples is adopted to extract the visual response toward color graininess. We also propose a periodic color halftone removing algorithm based on *Short Time Fourier Transform* to preprocess the scanned color patches. We demonstrate that the algorithm selectively removes only the **AM** halftone signals with minimal impact on other signals including **FM** halftone signals.

The inherent nature of excessive chromatic low-pass response in human visual contrast sensitivity functions suggests the luminance variation to be the dominant factor in determining the perceived color graininess. After averaging the observers' responses on all color patches, we extract a logarithmic relationship between the objective color granularity metric and the perceived color graininess. This can be explained by the *Fechner's law* which governs a significant portion of compressive stimulus sensitivities of human perception.

References

[1] Yee Ng, Chunghui Kuo and Di Lai, "Perceptual Color Graininess of Printed Pages via Flatbed Scanner", IS&T ICIS'06, pp.122-125, 2006.

[2] W. Kress, "Digitization and Metric Conversion for Image Quality test targets", 'IS&T PICS2003, pp.82-87, 2003.

[3] Chunghui Kuo and Yee Ng, "Image Graininess via flatbed scanner and image segmentation", IS&T NIP21, pp.84-88, 2005.

[4] G. Casella and R. Berger, "Statistical Inference, 2nd Ed.", Duxbury Press, 2001.

[5] ISO/IEC13660, "Information technology-office equipment-Measurement of image quality attributes for hardcopy output-Binary monochrome text and graphic images", 2001.

[6] M. Fairchild, "Color Appearance Model, 2nd Ed.", Wiley, 2005.

[7] T. Bouk and N. Buringham, "Measurement of graininess for halftone electrophotography", Proc. IS&T NIP8, pp.506-509, 1992.

Author Biography

Chunghui Kuo received his Ph.D. in Electrical and Computer Engineering from University of Minnesota and joined NexPress Solutions Inc. (a Kodak Company) since 2001. His research interest is in image processing, image quality, blind signal separation and classification, and neural network applied in signal processing. He is a Senior Member of IEEE signal processing society and a member of IS&T and SPIE.

Yee S. Ng is a Senior Research Associate and Intellectual Property Coordinator for NexPress Solutions, Inc. (a Kodak Company). He was Chief Engineer with responsibility for the engine image chain and image quality before that. He was a Science Associate and Project Chief Engineer at Eastman Kodak Company before joining NexPress in 1998. He is a Kodak Distinguished Inventor and holds 88 US patent. He is a Fellow of IS&T and a Senior Member of IEEE. He is a member of New York Academy of Sciences and APS. He is Project Editor for ISO/IEC 19799 (Gloss Uniformity), and Convener of WG03 (productivity) for ISO/IEC JTC1 SC28 (Office Equipment) and Liaison officer from SC28 to ISO/IEC TC130 (Graphics). He was General Chairman of NIP19 and received the Chester Carlson Award from IS&T in year 2000.